Electronic Supplementary Material (ESI) for Journal of Materials Chemistry C.
This journal is © The Royal Society of Chemistry 2023

Micro-patterned $BaTiO_3$@Ecoflex Nanocomposite Assisted Self-powered and Wearable Triboelectric Nanogenerator with Improved Charge Retention by 2D $MoTe_2$/PVDF Nanofibrous Layer

Debmalya Sarkar[1], Namrata Das[1], Souvik Sau[1, 3], Ruma Basu[2], Sukhen Das[1*]*

1 Department of Physics, Jadavpur University, Kolkata 700032, West Bengal, India.

2 Department of Physics, Jogamaya Devi College, Kolkata 700026, West Bengal, India.

3 Department of Physics, Bangabasi College, Kolkata 700009, West Bengal, India.

*Corresponding authors:

Sukhen Das (sdasphysics@gmail.com Mob: +919433091337)

Ruma Basu (ruma.b1959@gmail.com Mob: +919433115930)

1. Flexibility and weight of EPMTNG device:

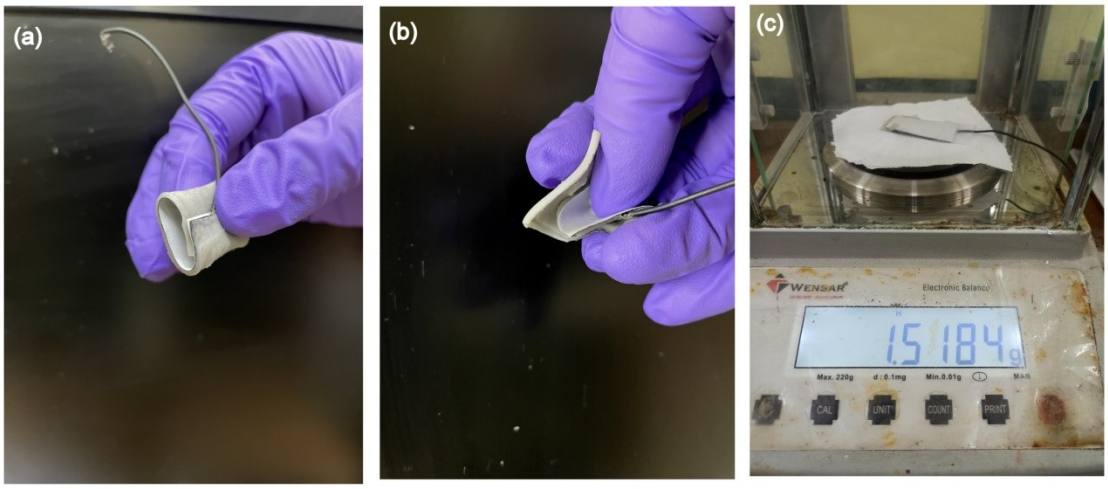

Figure S1: The flexibility of device at (a) rolling and (b) twisting mode. (c) Weight measurement of EPMTNG device.

2. Synthesis method of $BaTiO_3$ (BTO):

The nanoparticles were synthesized by simple hydrothermal process. At first, 2g Barium hydroxide salt was measured and dissolved it in 100mL double distilled water. Thereafter, 0.5g Titanium dioxide salt was added with the solution and placed it on a magnetic stirrer for 2h to dissolve the salts totally. In the next step, the solution was transferred in a hydrothermal setup and placed it in a vacuum oven at 160^{o}C for 4h. After that the hydrothermal set up was cooled down and centrifugation process was performed. Thereafter, the collected product after centrifugation was dried in a vacuum oven for 12h at 60^{o}C. In the final step, the synthesized powders were heat treated in air at 500^{o}C for 1h.

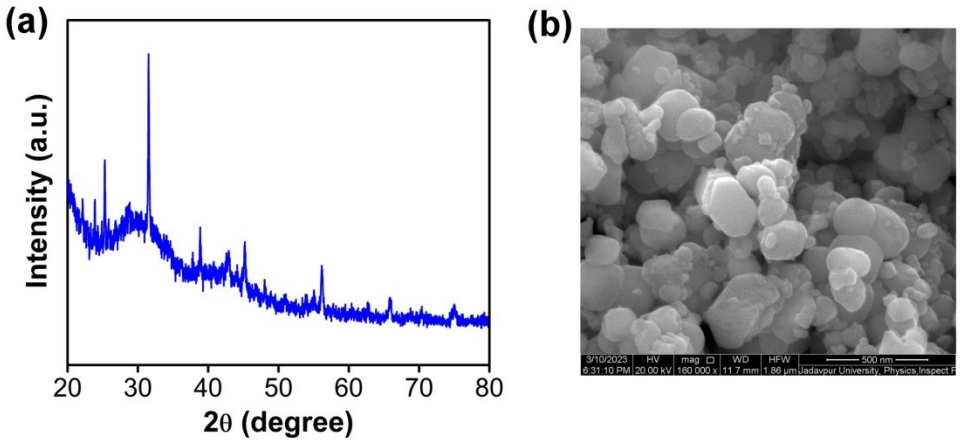

Figure S2: (a) Diffraction peaks of BTO nanoparticles. (b) Surface morphology of synthesized nanoparticles.

3. Synthesis method of 2D $MoTe_2$ (MT) nanoparticles:

Firstly, 1.088g Sodium molybdate dehydrate, 1.148g metal Tellurium powder and 0.255g Sodium borohydride were mixed with 60mL double distilled water at room temperature under continuous stirring condition. After that, the mixture was poured in a hydrothermal set up and performed the hydrothermal process at 200^0C for 30h. Thereafter, the samples were collected and cleaned thoroughly with distilled water and acetone. Then the cleaned sample was dried at 60^0C to obtain the MT nanoparticles.

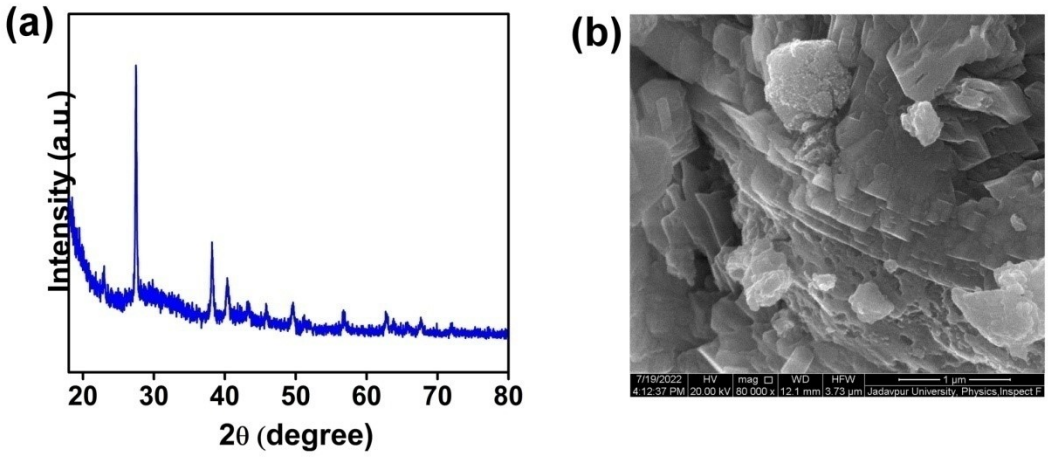

Figure S3: (a) Crystalline peaks of MT nanoparticles. (b) Layered structure of synthesized nanoparticles from FESEM image.

4. Thickness dependent output performance and twisting test of EPMTNG device:

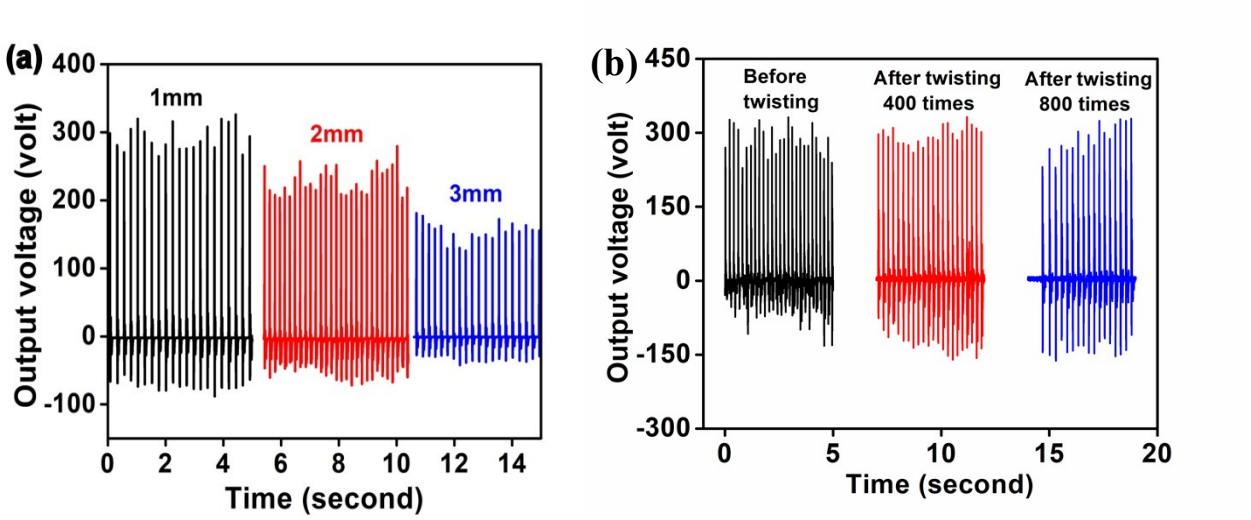

Figure S4: (a) Output voltage of EPMTNG device generated at different thickness of EBTO nanocomposite. (b) Twisting performance of the fabricated device

5. EDS spectrum and elemental mapping of EBTO nanocomposite and PM5 nanofibers

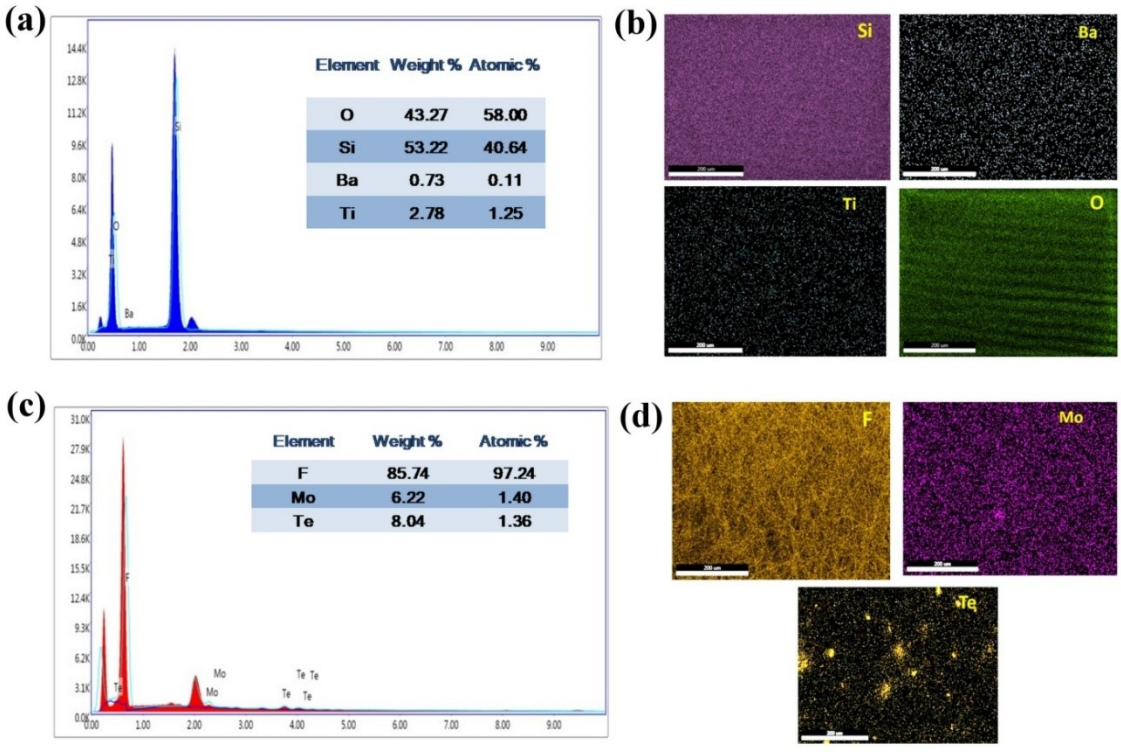

Figure S5: (a) EDS spectra and (b) elemental colour mapping of EBTO nanocomposite. (c) Energy dispersive spectrums and (d) elemental mapping of MT incorporated PVDF nanofibers.

6. Calculation of applied force of EPMTNG:

By using following two equations, the force which is applied on the EPMTNG device under periodic finger tapping has been calculated. These two equations depend on energy momentum conservation law.

$m.g.h = ½ mv^2$

or, $v = (2gh)^{1/2}$ …… (i)

$(F-mg).\Delta t = m.v$ …… (ii)

Where, **m** is the mass of the finger and **v** represents the velocity of finger when it touches EPMTNG device, **h** defines the height of the falling object (finger), **F** is the force which is applied on device, **g** is gravitational acceleration and **Δt** represents the duration of time between two consecutive positive or negative peaks deliberated from the output performance graph.

7. Electrical properties of charge generating and charge trapping layer:

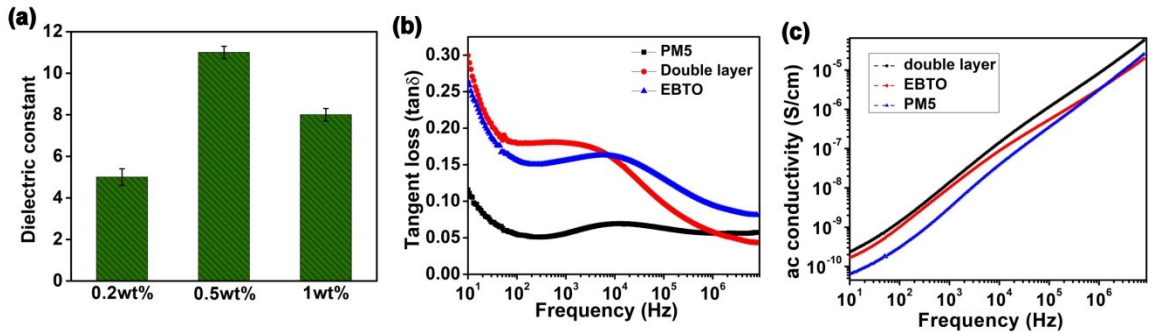

Figure S6: (a) Dielectric constant of EBTO layer at different weight percentage loading of BTO nanoparticles. (b) Tangent loss of EBTO layer, PM5 nanofiber and double layer. (c) Measured ac conductivity of three layers by varying frequencies.

8. Monitoring swallowing and speaking ability of device:

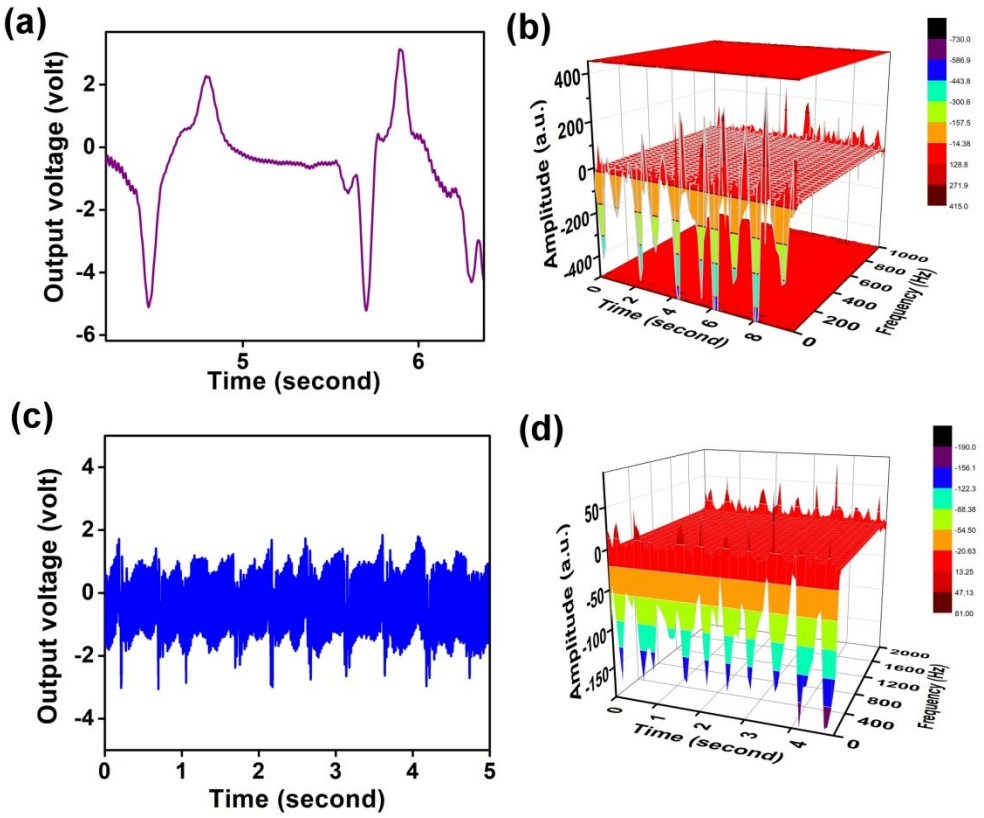

Figure S7: (a) Output voltage generation during swallowing. (b) STFT spectrogram of swallowing process. (c) Voltage generation by EPMTNG device from muscle movements at the time of speaking. (d) STFT spectrogram of speaking process**.**

9. Circuit diagram of illuminating LEDs and charging capacitors:

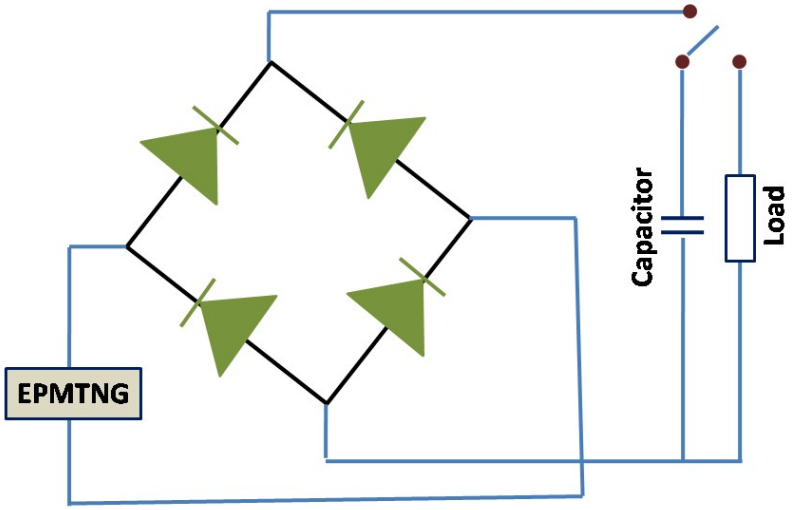

Figure S8: Circuit diagram of lighting up blue LEDs and charging three different capacitors.

10. Effect of surface modification of EBTO nanocomposite on output performance:

To improve the performance of triboelectric nanogenerator, surface modification plays a vital role. In this present work, 3D printed mould has been utilized to modify the surface of charge generating layer (EBTO nanocomposite), resulting in the micro-patterned surface of EBTO nanocomposite. The micro-patterned structure creates the surface roughness on EBTO nanocomposite and assists in increment of effective contact area between human hand and EBTO layer. Therefore, more triboelectric charges are induced on the surface of EBTO layer and human hand. As a result, potential difference increases during triboelectrification process, which accelerates the charge transfers among the carbon tape and ground state and leads in enhancement of output performance of EPMTNG device. The following equations can be used to explain the enhancement of output performance.[12]

$Q = \sigma.A$ ..... **(iii)**

$$V_{OC} = \frac{\sigma.x(t)}{\varepsilon_0}$$ **……. (iv)**

Where, Q is the transferred charge, $\boldsymbol{\sigma}$ represents the surface charge density, A is the effective contact area, V_{OC} defines the output voltage, $\boldsymbol{\varepsilon_0}$ is the free space permittivity and x(t) is the separation distance. With the increment of surface roughness of EBTO layer, effective contact area (A) also increases which will enhance the charge transfer (Q). According to equation (iii), the surface charge density and the contact area are proportional to the charge transfer. Thus, the surface charge density is linear to the contact area. Therefore, from equation (iv), it can be visualized that the increment of contact area induces more surface charge density which further assists in enhancement of output voltage of EPMTNG device.

11. Theoretical investigation of the effect of PM5 layer in charge loss:

The following equations help in establishing the idea of insertion of PM5 layer in EPMTNG device, which will be[12,14]

$$\varepsilon_r = \frac{d_{film} C_0}{A\, \varepsilon_0}$$ ..... (v)

$$P = \varepsilon_0(\varepsilon_r - 1)E$$ ……... (vi)

$$\sigma = \frac{V\varepsilon_0\varepsilon_r}{d}$$ ..... (vii)

$$V_{OC} = \frac{\sigma x(t)}{\varepsilon_0}$$ …….. (viii)

Where, $\boldsymbol{\varepsilon_r}$ defines the relative permittivity, d_{film} stands for the thickness of EBTO nanocomposite and PM5 layer, C_0 is the highest capacitance value, A defines the area of the EBTO nanocomposite and PM5 layer, $\boldsymbol{\varepsilon_0}$ represents the free space permittivity, P represents the polarization at electric field, E defines the electric field, $\boldsymbol{\sigma}$ is the surface charge density, V

represents the surface potential, d is the thickness of the device, V_{oc} defines the output voltage of the fabricated device and x(t) is the separation distance. With the addition of PM5 layer, the capacitance value of the device increases which helps in enlarging the relative permittivity from equation (v). Thus, the higher relative permittivity assists in strengthening the polarization effect under the application of electric field, illustrated in the equation (vi) and captures more triboelectric charges. Owing to this high permittivity and polarization effect, the PM5 layer reduces the charge loss and enhances the surface charge density of the device from equation (vii). As a result, the enhancement of the surface charge density improves the output voltage of EPMTNG device, described from equation (viii).

Table S1: Crystalline size and other parameters of BTO nanoparticles

Peak position (2θ)	FWHM (β)	Crystalline size (D) in nm	Microstrain	Dislocation density (δ) in nm^{-2}
23.38841	8.975	9.039199306	0.1891968	0.012238835
29.43656	5.564	14.76242074	0.0924203	0.004588649
36.8923	11.85	7.067140747	0.1550151	0.020022233
43.21281	5.422	15.75927335	0.0597336	0.004026499
47.83022	8.824	9.848576431	0.0868228	0.010309867
56.23773	16.859	5.342795575	0.1376589	0.035031835
66.46394	10.397	9.134872987	0.0692414	0.011983812
77.39912	22.904	4.444335604	0.1247444	0.05062748

Table S2: Crystalline size and other structural parameters of MT nanoparticles

Peak position (2θ)	FWHM (β)	Crystalline size (D) in nm	Microstrain	Dislocation density (δ) in

				nm^{-2}
27.48546	0.28717	28.47936409	0.0051235	0.001232933
38.21063	0.32076	26.2108107	0.0040405	0.00145559
40.36877	0.38304	22.09715331	0.0045464	0.002047988
45.85212	0.12221	50.58050087	0.0012608	0.00039087
49.57632	0.24608	35.55968099	0.002325	0.000790832

Table S3: Comparison of output performance of EPMTNG device with previously reported 2D material based TENGs and nanofibers based TENGs.

TENG based on 2D materials and nanofibers	**Operating mode**	**Open circuit voltage**	**Short circuit current or current density**	**Power or power density**
Metal–Organic Framework: A Novel Material for Triboelectric Nanogenerator–Based Self-Powered Sensors and Systems[1]	Contact-separation	164V	7μA	392mW/m^2
Highly conductive 1D-2D composite film for skin-mountable strain sensor and stretchable triboelectric nanogenerator[2]	Single electrode	95.8V		160mW/m^2
2D Materials-Based Electrochemical Triboelectric Nanogenerators[3]	Contact-separation	300V		530mW/m^2

Facile method to enhance output performance of bacterial cellulose nanofiber based triboelectric nanogenerator by controlling micro-nano structure and dielectric constant[4]	Contact-separation	181V	21μA	4.8W/m^2
UV-Protective, Self-Cleaning, and Antibacterial Nanofiber-Based Triboelectric Nanogenerators for Self-Powered Human Motion Monitoring[5]	Contact-separation			48.mW/m^2
Honeycomb-like nanofiber based triboelectric nanogenerator using self-assembled electrospun poly(vinylidene fluoride-co-trifluoroethylene) nanofibers[6]	Contact-separation	160V	17μA	1.6W/m^2
Characterization of PI/PVDF-TrFE Composite Nanofiber-Based Triboelectric Nanogenerators Depending on the Type of the Electrospinning System[7]	Contact-separation	364V	17.2μA	2.56W/m^2

Seed Power: Natural Seed and Electrospun Poly(vinyl difluoride) (PVDF) Nanofiber Based Triboelectric Nanogenerators with High Output Power Density[8]	Contact-separation	84V		334mW/m^2
Deep Trap Boosted Ultrahigh Triboelectric Charge Density in Nanofibrous Cellulose-Based Triboelectric Nanogenerators[9]	Contact-separation		8.2μA	3.83mW
Nafion-mediated barium titanate-polymer composite nanofibers-based triboelectric nanogenerator for self-powered smart street and home control system[10]	Contact-separation	307V	1.8μA/cm^2	1.12mW/m^2
Flexible composite-nanofiber based piezo-triboelectric nanogenerators for wearable electronics[11]	Contact-separation	42V	1.7mA/m^2	161.7mW/m^2
Our present work	**Single electrode**	**319V**	**9mA/m^2**	**2.9W/m^2**

VS1: Video of illuminating blue LEDs under finger pressing condition.


LED illumination.mp4

References:

1. Khandelwal, G.; Chandrasekhar, A.; Maria Joseph Raj, N. P.; Kim, S. J. Metal–organic framework: a novel material for triboelectric nanogenerator–based self-powered sensors and systems. Advanced Energy Materials 2019, 9, 1803581.

2. Lan, L.; Yin, T.; Jiang, C.; Li, X.; Yao, Y.; Wang, Z.; Qu, S.; Ye, Z.; Ping, J.; Ying, Y. Highly conductive 1D-2D composite film for skin-mountable strain sensor and stretchable triboelectric nanogenerator. Nano Energy 2019, 62, 319-28.

3. Pace, G.; del Rio Castillo, A. E.; Lamperti, A.; Lauciello, S.; Bonaccorso, F. 2D Materials-based Electrochemical Triboelectric Nanogenerators. Advanced Materials 2023, 26, 2211037.

4. Shao, Y.; Feng, C. P.; Deng, B. W.; Yin, B.; Yang, M. B. Facile method to enhance output performance of bacterial cellulose nanofiber based triboelectric nanogenerator by controlling micro-nano structure and dielectric constant. Nano Energy 2019, 62, 620-7.

5. Jiang, Y.; Dong, K.; An, J.; Liang, F.; Yi, J.; Peng, X.; Ning, C.; Ye, C.; Wang, Z. L. UV-protective, self-cleaning, and antibacterial nanofiber-based triboelectric nanogenerators for self-powered human motion monitoring. ACS Applied Materials & Interfaces 2021, 13, 11205-14.

6. Jang, S.; Kim, H.; Kim, Y.; Kang, B. J.; Oh, J. H. Honeycomb-like nanofiber based triboelectric nanogenerator using self-assembled electrospun poly (vinylidene fluoride-co-trifluoroethylene) nanofibers. Applied Physics Letters 2016, 108(14).

7. Kim, Y.; Wu, X.; Lee, C.; Oh, J. H. Characterization of PI/PVDF-TrFE composite nanofiber-based triboelectric nanogenerators depending on the type of the electrospinning system. ACS Applied Materials & Interfaces 2021, 13, 36967-75.

8. Singh, S. K.; Kumar, P.; Magdum, R.; Khandelwal, U.; Deswal, S.; More, Y.; Muduli, S.; Boomishankar, R.; Pandit, S.; Ogale, S. Seed power: natural seed and electrospun Poly (vinyl difluoride)(PVDF) nanofiber based triboelectric nanogenerators with high output power density. ACS Applied Bio Materials 2019, 2, 3164-70.

9. Wang, N.; Yang, D.; Zhang, W.; Feng, M.; Li, Z.; Ye, E.; Loh, X. J.; Wang, D. Deep trap boosted ultrahigh triboelectric charge density in nanofibrous cellulose-based triboelectric nanogenerators. ACS Applied Materials & Interfaces 2022, 15, 997-1009.

10. Pandey, P.; Jung, D. H.; Choi, G. J.; Seo, M. K.; Lee, S.; Kim, J. M.; Park, I. K.; Sohn, J. I. Nafion-mediated barium titanate-polymer composite nanofibers-based triboelectric nanogenerator for self-powered smart street and home control system. Nano Energy 2023, 107, 108134.

11. Wu, Y.; Qu, J.; Daoud, W. A.; Wang, L.; Qi, T. Flexible composite-nanofiber based piezo-triboelectric nanogenerators for wearable electronics. Journal of Materials Chemistry A 2019, 7, 13347-55.

12. Xie, X.; Chen, X.; Zhao, C.; Liu, Y.; Sun, X.; Zhao, C.; Wen, Z. Intermediate layer for enhanced triboelectric nanogenerator. Nano Energy 2021, 79, 105439.

13. Paria, S.; Bera, R.; Karan, S. K.; Maitra, A.; Das, A. K.; Si, S. K.; Halder, L.; Bera, A.; Khatua, B. B. Insight into cigarette wrapper and electroactive polymer based efficient TENG as biomechanical energy harvester for smart electronic applications. ACS Applied Energy Materials. 2018, 1, 4963-75.

14. Park, H. W.; Huynh, N. D.; Kim, W.; Lee, C.; Nam, Y.; Lee, S.; Chung, K. B.; Choi, D. Electron blocking layer-based interfacial design for highly-enhanced triboelectric nanogenerators. Nano Energy 2018, 50, 9-15.